sciendo

ARTIFICIAL SATELLITES, Vol. 59, No. 3 – 2024
DOI: 10.2478/arsa-2024-0007

ANALYSIS OF COMPARABILITY OF PCV IN SURVEYING-GRADE GNSS ANTENNA – TOPCON HIPER-VR CASE STUDY

Radosław BARYŁA, Karol DAWIDOWICZ

University of Warmia and Mazury in Olsztyn, Department of Geodesy,
Oczapowskiego 1, 10-719 Olsztyn, Poland

e-mails: radoslaw.baryla@uwm.edu.pl, karol.dawidowicz@uwm.edu.pl

ABSTRACT. It is well known that the phase center of a Global Navigation Satellite System (GNSS) antenna is not a stable point. For any given GNSS antenna, the phase center will change with the direction of the incoming signal from a satellite, as well as the frequency. Ignoring these phase center variations (PCVs) in GNSS data processing can lead to notable errors, especially in vertical position component determination. To avoid the problem, antenna PCV together with the phase center offset (PCO) information are recommended to be used in GNSS observation processing. We currently distinguish between individual and type-mean phase center correction (PCC) models. These models describe the variations in the phase center of the antenna as a function of the elevation angle and azimuth. In general, the primary difference between individual and type-mean models lies in their specificity. Individual models are highly precise but are valid only for a particular antenna model, while the type-mean models are more general and can be applied to a broad range of antennas of the same type, but may suffer from a lower level of precision. This paper aims to analyze the comparability of PCV in surveying-grade GNSS antennas. For the analyses, we propose to use an originally designed bench with precisely defined relative positions of the seven antenna mounting points. Preliminary studies have been performed using GPS observations on L1 and L2 frequencies recorded by seven Topcon HIPER-VR antennas. The results proved that the comparability of PCV for this antenna is high. The position error did not exceed 3 mm. It could be assumed that the type-mean PCC model could describe PCV all antennas of this type with good accuracy.

Keywords: antenna phase center variations, antenna phase center corrections, GPS, GNSS

1. INTRODUCTION

The phase center of a Global Navigation Satellite System (GNSS) antenna is the point within the antenna where the signals are received. It is not a fixed point, but can vary depending on different factors, including the elevation angle, azimuth, and signal frequency. Variations in the antenna's phase center can introduce errors in the calculated positions (Schön and Kersten 2014). These errors can affect both the horizontal and vertical components of the positioning solution. To avoid the problem, antenna phase center correction (PCC) models are recommended to be used in GNSS data processing. We can distinguish between so-called individual and type-mean PCC models. These models describe the variations in the antenna's phase center as a function of the elevation angle and the azimuth of the incoming GNSS signal.

Individual PCC models are valid for a particular GNSS antenna and are typically determined through extensive calibration and testing of one specific antenna piece. Individual PCC models are the most precise, but can be less convenient as they require calibration of a particular antenna, which can be quite expensive as there are only a few research centers in the world addressing this issue. Type-mean PCC models are more generalized and represent the average PCCs for a particular type or class of GNSS antennas. Type-mean PCC models are more convenient because they do not provide specific data for individual antennas. Instead, they provide a model that can be applied to any antenna of the same type. However, they may not be as accurate as individual models since they do not capture the specific characteristics of each antenna.

The PCC can be obtained either from measurements performed in anechoic chambers, according to Gorres et al. (2006) or Zeimetz and Kuhlman (2008), or through field calibrations (Wübbena et al. 2006). In recent times, the standard procedure for field calibration, developed by the Institut für Erdmessung (IfE; Leibniz Universität Hannover) and Geo++ company (Wübbena et al. 1997), involves the use of a robot. In its initial concept, this approach was assumed to generate sidereal time differences in observations, which required a minimum of 2 days of measurements to calibrate a single antenna. Mader (1999) presented a relative calibration system that was subsequently embraced by the International GNSS Service (IGS) for its initial network processing. Over time, this technique has undergone enhancements, including the reduction of calibration time through the implementation of a robotic mechanism that rotates the calibrated antenna (Wübbena et al., 2000; Bilich and Mader, 2010). By rotating the antenna, its phase behavior can be separated from the reference antenna, and consequently, this enables the creation of so-called absolute PCC. The calibration technique using robots is intensively developing. This is manifested through new calibration centers (Willi et al. 2020, Wübbena et al. 2019, Dawidowicz et al. 2021, Tupek et al. 2023) or the inclusion of new GNSS signals in the calibration process (Kröger et al. 2021, Wanninger et al. 2022).

Validating the PCC for a GNSS antenna is crucial to guarantee the correction models' precision and dependability. Various methods and approaches have been devised to accomplish this objective. Cross-validation with independent sources stands out as a particularly direct approach for PCC validation. In this approach, we can assess the antenna's performance by comparing it with data obtained from independent sources. In the subsequent step, the differences in position components calculated using these different PCC models are compared. Further information and illustrative results can be found in papers such as Dawidowicz (2011), Araszkiewicz and Völksen (2016), Krzan et al. (2020), and Araszkierwicz and Kiliszek (2020). An alternative variation of this approach includes analyzing the repeatability of the long-term stability of PCC by conducting repeated field measurements over a period of time. This can be done by, for example, monitoring the antenna's performance to check for consistency and any potential changes in the corrections due to factors like antenna swapping on the station or antenna aging (Dawidowicz et al. 2023). Bergsted et al. (2020) assessed the performance of GNSS absolute antenna calibrations and their effect on precise positioning. They introduced a novel evaluation method that combines inter-antenna differentials with laser tracker measurements. Borowski et al. (2022) proposed assessing the appropriateness of antenna PCC variations by examining a vital component known as the phase center offset (PCO) of the antennas. To achieve this objective, the authors employed diverse and independent approaches to determine the discrepancies in height. These methods included the EUREF Permanent Network (EPN) combined solutions, precise point positioning (PPP), and the single baseline solution. The outcomes obtained from GNSS processing were then compared to the outputs of direct geometric leveling, facilitating the derivation of meaningful conclusions. Kersten et al. (2022) observed that there are noteworthy disparities in the antenna patterns, which necessitate

a comprehensive examination and a robust comparative framework to assess their effect on geodetic parameters accurately. These parameters include station coordinates, zenith wet delays, and receiver clock estimates. In the study, the authors propose a novel approach for evaluating calibration values of receiver antennas. They introduce novel scalar metrics and emphasize their advantages and significance in the analysis. Kallio et al. (2018) introduced a captivating approach to authenticate the accuracy of antenna calibration tables through a field test procedure. The concept, known as Revolver, was inspired by the permutation method, wherein antennas were systematically rotated to ensure that each antenna visited every test site at least once. In the proposed method, antennas are usually oriented to the North; however, during certain sessions and in specific pillars, the antennas are rotated by 180°. The arrangement and rotation of antennas may differ based on the number of antennas and pillars utilized during testing. The researchers demonstrated that the suggested approach allows for determining the residual offsets in the antenna at a sub-millimeter scale.

In the paper, we present a field test method for analysis of comparability of phase center variation (PCV) in GNSS antenna. We propose to use an originally designed bench with precisely defined relative positions of the seven antenna mounting points. Analysis of the results of the GNSS measurements performed on the bench allows the determination of the spatial vectors of displacements from the reference position for each tested antenna and, in this way, the validation of the comparability of PCV.

2. PCV SPECIFICATION OF THE TOPCON HIPER-VR ANTENNA

For the proposed method of validation, we used seven surveying-grade antennas of the same type, that is, Topcon HIPER-VR one (Figure 1). Table 1 presents details of the Topcon HIPER-VR PCO derived from igs20_2239.atx file.

Figure 1. Topcon HIPER-VR antenna

Table 1. Topcon HIPER-VR antenna PCO for the Global Positioning System (GPS) signals

Antenna model	GPS L1 PCO (mm)			GPS L2 PCO (mm)		
	N	E	U	N	E	U
TPSHIPER_VR NONE	3.26	–2.87	58.67	4.85	3.18	52.76

Topcon HIPER-VR antenna has full-phase center position information for GPS and GLObalnaya NAvigatsionnaya Sputnikovaya Sistema (GLONASS) signals obtained from absolute calibrations (Figure 2). On analyzing data presented in Figure 2, it is found that the smallest PCV values, not exceeding 5 mm, are revealed for the GPS L1 frequency. However, the largest spread of PCV values, from –8 to 8 mm, is seen in the case of GPS L2 frequency.

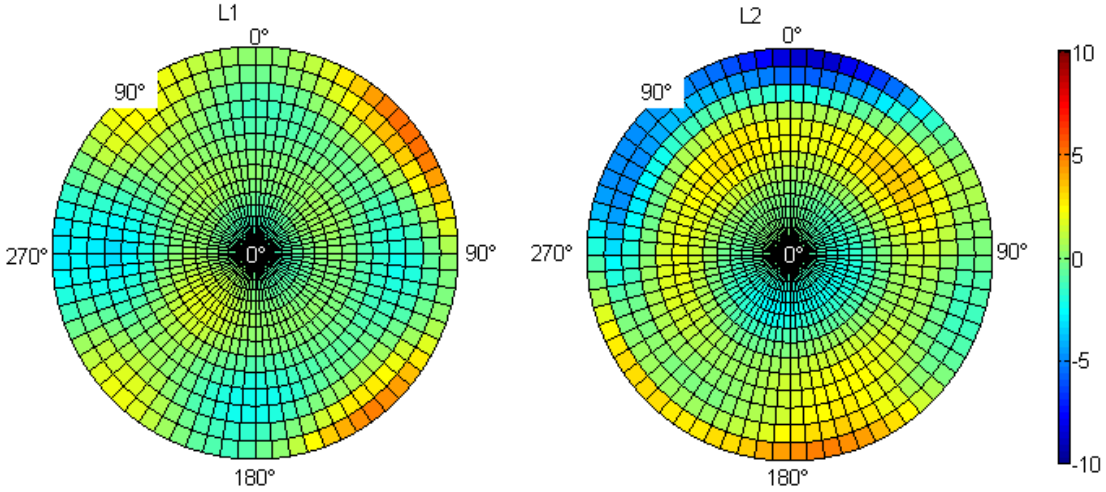

Figure 2. TPSHIPER_VR NONE antenna PCV patterns for GPS L1 and L2 signals (mm)

3. METHODOLOGY AND EXPERIMENT DESIGN

We usually use available GNSS receivers and antennas to perform static measurements on points in a geodetic network. Nonintegrated and integrated GNSS receivers and antennas of various types can be used in such measurements. The final results are obtained at the post-processing stage. One of the requirements for high accuracy is the use of, preferably, individual, PCC models of receiver antennas. Individual models are highly precise and unique to a single antenna piece, but obtaining them is time-consuming and expensive. Therefore, a good approximation of the individual model may be a type-mean one. In order for such a model to fulfill its purpose well, the compatibility of PCV for all antennas of the same type should be high.

The compatibility of PCV was verified on a test bench (Baryła et al. 2023). The proposed solution allows the tested GNSS antennas to be positioned horizontally, in a single line, and at equal intervals. Such a system allows a simple local coordinate system to be realized based on a straight-line function, thus generating theoretical coordinates of the GNSS antennas. A representative volume of Topcon HIPER VR GNSS receivers integrated with the antennas was used in the experiment (Table 2, Figure 3). Seven units were considered to be a sufficient number as the type-mean model of the TPSHIPER_VR NONE antenna has been created based on the calibration results of five antennas.

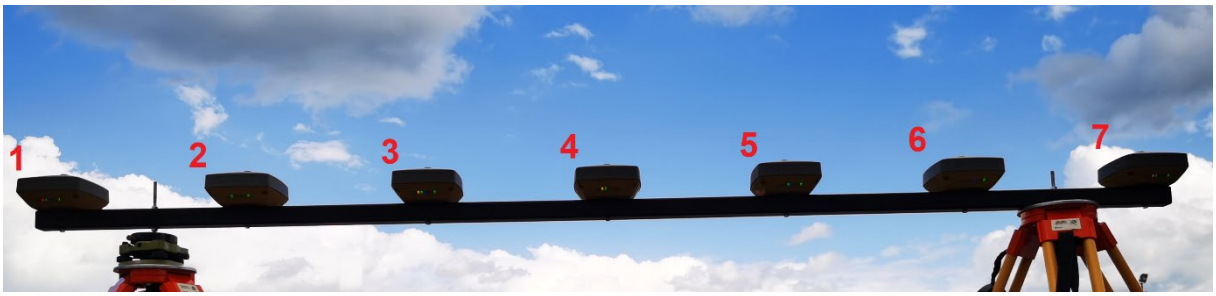

Figure 3. TPSHIPER_VR NONE antennas on a test bench

The mounting method on the test bench ensures the correct orientation of the antenna. The antennas under test were positioned at the same height in a single line oriented in the North–South direction, at equal intervals of 0.4000 m. Static GNSS observations were recorded on September 3, 2023 for 6 h, starting from 13:00 UTC. We have decided that a 6-h measurement session (half of the period of repeatability of the GPS constellation) is sufficient to validate the type-mean antenna PCC model using the proposed approach. Measurements were carried out with an interval of 1 s, using an elevation mask of 0°. Due to the short length of the bench, it can be assumed that all tested antennas were in similar field conditions. In addition, an elevation mask of 10° was adopted to post-process the observations to minimize the possible impact of multipath (MP) on final results. Finally, the stability of the test bench was checked by their height verification before and after the measurement. It should be noted that there was no change in the height of the test system during the measurements.

Table 2. Topcon HIPER-VR antenna serial numbers

Antenna test #	Antenna serial #
1	1451-10176
2	1451-10191
3	1451-10214
4	1451-10217
5	1451-10895
6	1449-12775
7	1449-12778

The collected GNSS observations were converted to RINEX 3.04 format. Post-processing was done using RTKLib 2.14 software by determining the satellite vectors (SVs) between GNSS benchmark antenna #**1** and the other antennas. Geocentric coordinates in the PL-ETRF 2000 system of point no. **1** were determined on the basis of ASG-EUPOS with reference to the nearest permanent GNSS station located in Olsztyn (OPNT), 2.2 km away. The selected options and parameters of the data processing with the RTKLib software are summarized in Table 3.

Table 3. RTKLib processing options

Parameter	Setting
Positioning mode	Baseline – static
Constellation	GPS
Observations	L1+L2 code and phase
Elevation cut-off angle	10°
Ephemeris	Broadcast
Ionospheric delay handling	Broadcast
Troposphere delay handling	Saastamoinen
Ambiguity handling	Fix and hold with LAMBDA algorithm
Receiver antenna PCV corrections	igs20_2239.atx
Session length	6 h

We used GPS-only signals to verify the comparability of PCV of the TOPCON HIPER-VR antenna. First of all, in the type-mean PCC model of the TOPCON HIPER-VR antenna, only GPS and GLONASS correction for L1 and L2 frequencies were available. In addition, the antenna calibration for GLONASS signals differed in comparison to GPS because of the different frequencies of individual GLONASS satellites. During antenna calibration, the PCCs for both signals were created from the mixture of observed GLONASS frequencies. For this reason, the calibration results are satellite constellation dependent and are not as accurate as for GPS, which is reported by some researchers (Wübbena et al. 2006). As our intention was to check if the type-mean PCC could describe the PCV of surveying-grade GNSS antenna in the optimal case, we decided to reduce our analysis to GPS-only data.

4. METHODOLOGY AND RESULTS IN POSITION DOMAIN

The vector coordinates obtained from GPS data processing, with reference to point **# 1**, were used to determine coordinates in the PL-ETRF 2000 system. The coordinates of all points were transformed to the local topocentric system with the fixed point **# 1**, resulting in plane coordinates *n* and *e* and vertical component *u*. By defining the primary system as a straight-line function, realized by the test bench, a spatially indeterminate system was obtained, which makes it impossible to perform the seven-parameter Helmert transformation. Therefore, two independent systems were introduced with the fixed point **# 1** (0, 0, 0): horizontal, in which the *n* components for successive points increase with an interval of 0.4000 m, while the coordinates *e* for all points are equal to zero, and a vertical one in which all points were located at heights equal to zero. The realization of the secondary systems are the position components from post-processing: for the horizontal system, the *N* and *E*, and for the vertical system, the *U*.

Horizontal corrections *dn* and *de* to the Antenna Reference Point (ARP) of the GNSS antennas were obtained from the 2D Helmert similarity transformation. The transformation coefficients were determined by taking all the measured points as fixed. Denoting the set of points of the primary system (n_i, e_i) and the set of points of the secondary system (N_i, E_i), where i = 1, 2, …, k, the coordinates of the centers of balance in both systems were calculated (Kadaj, 2002), assuming the number of observations k = 7:

$$n_0 = (\Sigma n_i)/k \ , e_0 = (\Sigma e_i)/k \ , N_0 = (\Sigma N_i)/k \ , E_0 = (\Sigma E_i)/k. \quad (1)$$

In the next step, all coordinates were recalculated using formulas:

$$\underline{n_i} = n_i - n_0, \underline{e_i} = e_i - e_0, \underline{N_i} = N_i - N_0, \underline{E_i} = E_i - E_0. \quad (2)$$

The transformation coefficients C and S were determined from:

$$C = W_1/W \quad (3)$$

$$S = W_2 - W \quad (4)$$

$$W = \Sigma\left(\underline{n_i}^2 + \underline{e_i}^2\right) \quad (5)$$

$$W_1 = \Sigma\left(\underline{N_i} \cdot \underline{n_i} + \underline{E_i} \cdot \underline{e_i}\right) \quad (6)$$

$$W_2 = \Sigma\left(\underline{N_i} \cdot \underline{n_i} - \underline{E_i} \cdot \underline{e_i}\right) \quad (7)$$

In the next stage, the conversion of coordinates from the primary system *n*, *e* to the secondary system *N'*, *E'* was performed:

$$N_i' = N_0 + C \cdot \underline{n_i} + S \cdot \underline{e_i} \quad (8)$$

$$E_i' = E_0 + C \cdot \underline{n_i} + S \cdot \underline{e_i} \quad (9)$$

The determined components of the displacement vector are the differences between the coordinates from the GNSS observation post-processing and the coordinates after transformation (Figure 4):

$$dn_i = N_i - N_i' \quad (10)$$

$$de_i = E_i - E_i' \quad (11)$$

On the basis of the above results, the transformation error was estimated with $f = k = 7$, which equal $m_t = 1.1$ mm:

$$m_t = \sqrt{\Sigma(dn_i^2 + de_i^2)/f} \quad (12)$$

In the case of the obtained heights *u*, the arithmetic mean satisfying the condition that the sum of residuals reaches minimum was taken as the true value. By differentiation of the values of the individual heights with the mean value, the *du* components of the displacement vector were obtained (Figure 4):

$$U_0 = (\Sigma U_i)/k \quad (13)$$

$$du_i = U_i - U_0 \quad (14)$$

Generally, it can be assumed that obtained dn_i, de_i, and du_i residuals are a consequence of individual differences in the antenna phase centers, differences in MP, and measurement noise. However, due to the short length of the bench, all tested antennas were in similar field conditions and the impact of MP is almost entirely reduced using the relative positioning model for a short baseline. For this reason, it can be assumed that possible notable differences visible in the obtained residuals may indicate that the type-mean PCC model is not able to describe the PCV of every single antenna precisely.

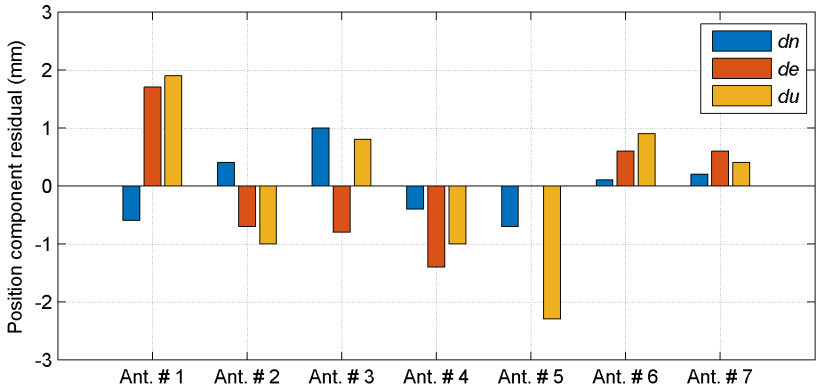

Figure 4. Position components' residuals

Our results (Fig. 4) proved that the type-mean PCC model of the Topcon HIPER-VR antenna correctly describes changes in phase center position. The position error due to the use of this type of antenna did not exceed 3 mm. On analyzing the results obtained for individual antennas, it is found that in the case of four antennas, specifically # 2, 3, 6, and 7, differences do not exceed 1 mm for all position components. In the case of antenna # 4 for the East component, the difference equaled 1.4 mm. The biggest differences occurred for antennas # 1 and 5. For antenna # 1, corrections for East and Up position components reached up to 2 mm. In the case of antenna # 5, the biggest difference occurred, which equals 2.3 mm for the Up position component. An interesting phenomenon was also observed: similar correction values for the two newest antennas (# 6, 7) with serial numbers starting with "1449."

5. MP ANALYSIS

To understand the achieved results better, in this part, we focus on the analysis of MP as well as the root mean square (RMS) of MP linear combinations for GPS L1 and L2 frequencies. MP was derived using the following equations (Vázquez et al. 2012):

$$\mathrm{MP1} = p_1 - \left(1 + \frac{2}{\alpha - 1}\right)\Phi_1 + \left(\frac{2}{\alpha - 1}\right)\Phi_2 \tag{15}$$

$$\mathrm{MP2} = p_2 - \left(\frac{2\alpha}{\alpha - 1}\right)\Phi_1 + \left(\frac{2\alpha}{\alpha - 1} - 1\right)\Phi_2 \tag{16}$$

where:

p_i – pseudo-range observation,

Φ_i – carrier phase observation,

$\alpha = \left(\frac{f_1}{f_2}\right)^2$

f_1 – frequency of L1, and

f_2 – frequency of L2.

We checked the potential differences in MP values for the employed antennas and whether these values correlated with the differences obtained in the position domain. Table 4 presents the mean RMSs of MP linear combination for all observed SVs for GPS L1 and L2 signals.

Table 4. Mean RMS of MP for GPS signals

Antenna test #	RMS of MP for L1 frequency (m)	RMS of MP for L2 frequency (m)
1	0.17	0.27
2	0.34	0.28
3	0.34	0.27
4	0.33	0.28
5	0.17	0.25
6	0.18	0.27
7	0.32	0.28

On analyzing the results presented in Table 4, it is found that for L1 frequency, the RMS of MP noticeably differs depending on the antenna unit. For this frequency, we can identify two groups of antennas: with test numbers 1, 5, and 6, where the RMS of MP obtains a value in the range from 0.17 to 0.18 m, and the other four antennas with RMS of MP that is in the range from 0.32 to 0.34 m (changes within a range of 100% between selected antennas from both groups). In the case of L2 frequency, the RMS of MP is more stable and achieves values from 0.25 to 0.28 m (changes within a range of 12%). We attribute this effect to the differences in MP reduction settings activated in receivers. In three cases (antenna # 1, 5, and 6) the MP reduction boxes have been enabled in the field of data collection, which was manifested by lower RMS of MP for GPS L1 frequency.

For detailed analysis, we chose one example satellite with a long observation window and all phases of the pass to be represented, that is, satellite ascending, culmination, and descending. In Figure 5 we present MP linear combination for GPS Satellite Vehicle (SV) 11. The results presented in Figure 5 clearly confirm our previous conclusion. Indeed, the MP values for L1 frequency obtained in the case of antennas #1, 5, and 6 are visibly smaller than those obtained for the other four antennas. However, we have not found a correlation between differences in MP values and the differences obtained in the position domain. We have also not found a correlation between the differences in GPS L1 MP values and Topcon HIPER-VR antenna serial numbers.

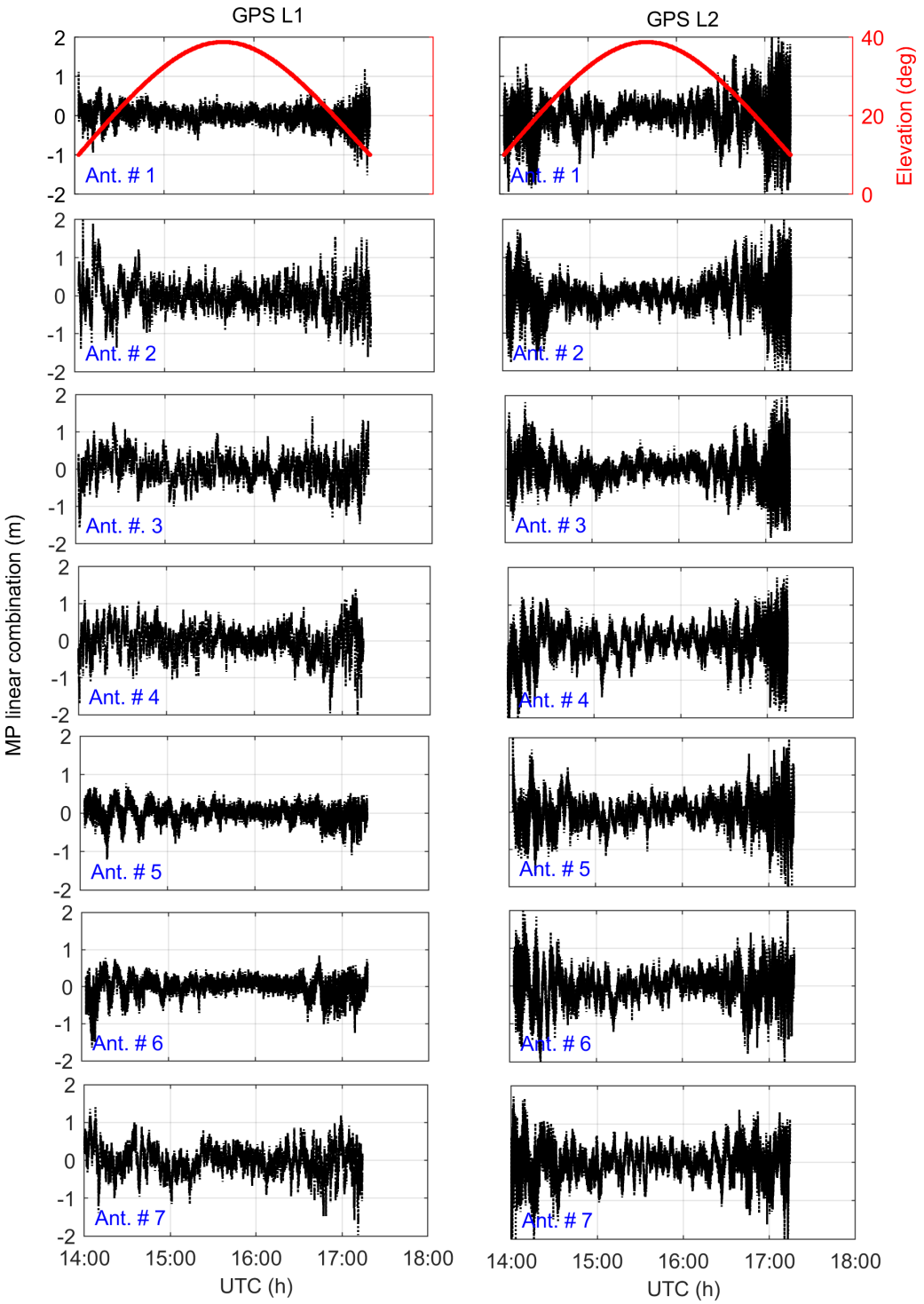

Figure 5. Multipath linear combination for GPS SV 11

6. CONCLUSIONS

In the paper, we analyzed the comparability of PCV of the Topcon HIPER VR antenna. To achieve our objective, we used in-house design construction consisting of a bench with precisely defined relative positions of the seven antenna mounting points. Preliminary tests were performed based on 6 h of GPS-only data post-processed using RTKLib software.

We proved that the type-mean PCC model for GPS L1 and L2 frequencies of the Topcon HiPer VR antenna could describe with good accuracy PCVs used in test seven Topcon antenna units. Such a conclusion can be justified because the comparability of PCV was high: values of spatial vector components of displacements from the reference position for each tested antenna did not exceed 3 mm.

It should be noted that we also analyzed the RMS of MP linear combinations for GPS L1 and L2 frequencies. The motivation for this part of the study was to check the potential differences in MP values for the different antennas and if these values correlated with the differences obtained in the position domain. We found that there is no correlation between differences in MP values and the differences obtained in the position domain.

Acknowledgements. Special thanks to Mr Michał Ogrodniczak of SKB GIS s.c. located in Olsztyn for his assistance in the field surveys and for sharing the observation data.

REFERENCES

Araszkiewicz A., Kiliszek D. (2020) Antenna Corrections for the Galileo E5a Frequency on Position Estimates, *Sensors*, Vol. 20, No. 19, 1-19, https://doi.org/10.3390/s20195536.

Araszkiewicz A., Völksen C. (2017) The impact of the antenna phase center models on the coordinates in the EUREF Permanent Network, *GPS Solutions*, Vol. 21, 747-757, https://doi.org/10.1007/s10291-016-0564-7.

Baryła R., Paziewski J., Wielgosz P. (2023) Vibration simulator of GNSS antennas, in particular for the purpose of determining terrain deformation, *Patent Office of the Republic of Poland*, Patent registration number: Ru.072933, https://ewyszukiwarka.pue.uprp.gov.pl/search/pwp-details/W.129623.

Bergstrand S., Jarlemark P., Herbertsson M. (2020) Quantifying errors in GNSS antenna calibrations: Towards in situ phase center corrections, *Journal of Geodesy*, Vol. 94, No. 105, https://doi.org/10.1007/s00190-020-01433-0.

Bilich A., Mader G. L. (2010) GNSS absolute antenna calibration at the National Geodetic Survey, *Proc. ION GNSS 2010,* Portland 2010, 1369-1377.

Borowski L., Kudrys J., Kubicki B. (2022) Phase Centre Corrections of GNSS Antennas and Their Consistency with ATX Catalogues, *Remote Sens*, eds. Slámová M., Maciuk K., Vol. 14, No. 3226, https://doi.org/10.3390/rs14133226.

Dawidowicz K. (2011) Comparison of using relative and absolute PCV corrections in short baseline GNSS observation processing, *Artificial Satellites*, 46 (1), 9-31, https://doi.org/10.2478/v10018-011-0009-z

Dawidowicz K., Krzan G., Wielgosz P. (2023) Offsets in the EPN station position time series resulting from antenna/radome changes: PCC type-dependent model analyses, *GPS Solutions*, Vol. 27, No. 9, https://doi.org/10.1007/s10291-022-01339-8.

Dawidowicz K, Rapiński J., Śmieja M., Wielgosz P., Kwaśniak D., Jarmołowski W., Grzegory T., Tomaszewski D., Janicka J., Gołaszewski P., Wolak B, Baryła R., Krzan G., Stępniak K., Florin-Catalin G., Brzostowski K (2021) Preliminary Results of an Astri/UWM EGNSS Receiver Antenna Calibration Facility, *Sensors*, Vol. 21, eds. https://doi.org/10.3390/s21144639.

Gürres B., Campbell M., Becker M. (2006) Absolute calibration of GPS antennas: laboratory results and comparison with field and robot techniques, *GPS Solutions*, eds. Siemes M., Vol. 10, 136-145, https://doi.org/10.1007/s10291-005-0015-3.

Kadaj R., (2002) Polskie układy współrzędnych formuły transformacyjne, algorytmy i program Link: http://www.geonet.net.pl/images/2002_12_uklady_wspolrz.pdf (accessed 20 November 2023)

Kallio U., Koivula H., Lahtinen S. (2019) Validating and comparing GNSS antenna calibrations, *Journal of Geodesy*, eds. Nikkonen V., Poutanen M., Vol. 93, 1-18, https://doi.org/10.1007/s00190-018-1134-2.

Kersten T., Kröger J., Schön S. (2022) Comparison concept and quality metrics for GNSS antenna calibrations, *Journal of Geodesy*, Vol. 96, No. 48, https://doi.org/10.1007/s00190-022-01635-8.

Kröger J., Kersten T., Breva Y. (2021) Multi-frequency multi-GNSS receiver antenna calibration at IfE: Concept - calibration results - validation, *Advances in Space Research*, Vol. 68, 4932-4947, eds. Schön S., https://doi.org/10.1016/j.asr.2021.01.029.

Krzan G., Dawidowicz K., Wielgosz P. (2020) Antenna phase center correction differences from robot and chamber calibrations: the case study LEIAR25, *GPS Solutions*, Vol. 24, No. 44, https://doi.org/10.1007/s10291-020-0957-5.

Mader G. L. (1999) GPS Antenna Calibration at the National Geodetic Survey, *Journal of Geodesy*, Vol. 3, 50-58, https://doi.org/10.1007/PL00012780.

Schön S., Kersten T. (2014) Comparing antenna phase center corrections: challenges, concepts and perspectives. IGS AC Workshop 2014 Link: https://www.ife.uni-hannover.de/uploads/tx_tkpublikationen/IGS2014_schoenKersten.pdf (accessed 20 November 2023)

Tupek A., Zrinjski M., Švaco M. (2023) GNSS Receiver Antenna Absolute Field Calibration System Development: Testing and Preliminary Results, *Remote Sensing*, eds. Barković Đ., Vol. 15, No. 4622, https://doi.org/10.3390/rs15184622.

Vázquez B, Guadalupe E, Grejner-Brzeziska D (2012) A case of study for Pseudorange multipath estimation and analysis: TAMDEF GPS network, Geofis Int 51: 63-72. https://doi.org/10.22201/igeof.00167169p.2012.51.1.146

Wanninger L., Thiemig M., Frevert V. (2022) Multi-frequency quadrifilar helix antennas for cm-accurate GNSS positioning, *Journal of Applied Geodesy*, Vol. 16, No. 1, 25-35, https://doi.org/10.1515/jag-2021-0042.

Willi D., Lutz S., Brockmann E, (2020) Absolute field calibration for multi-GNSS receiver antennas at ETH Zurich, *GPS Solutions*, eds. Rothacher M., Vol. 24, No. 28, https://doi.org/10.1007/s10291-019-0941-0.

Wübbena G., Schmitz M., Menge F., (1997) A New Approach for Field Calibration of Absolute GPS Antenna Phase Center Variations, *Navigation - Journal of the Institute of Navigation*, eds. Seeber G., Völksen Ch., Vol. 44, 247-255, https://doi.org/10.1002/j.2161-4296.1997.tb02346.x.

Wübbena G., Schmitz M., Boettcher G. (2006) Absolute GNSS antenna calibration with a robot: repeatability of phase variations, calibration of GLONASS and determination of carrier-to-noise pattern, *Proceedings of the IGS Workshop: Perspectives and Visions for 2010 and beyond*, eds. Schumann C., Darmstadt 2006.

Wübbena G., Schmitz M., Menge F. (2000) Automated Absolute Field Calibration of GPS Antennas in Real-Time, *Proc. ION GPS 2000,* eds. Böder V., Seeber G., Salt Lake City 2000, 2512-2522.

Wübbena G., Schmitz M., Warneke A. (2019) Geo++ Absolute Multi-Frequency GNSS Antenna Calibration, *Proc. EUREF Analysis Center Workshop*, http://www.geopp.com/pdf/gpp_cal125_euref19_p.pdf, Warsaw 2019.

Zeimetz P., Kuhlman H. (2008) On the Accuracy of Absolute GNSS Antenna Calibration and the Conception of a New Anechoic Chamber, *FIG Working Week 2008*, https://www.fig.net/resources/proceedings/fig_proceedings/fig2008/papers/ts05g/ts05g_01_zeimetz_kuhlmann_2901.pdf, Stockholm 2008.

Received: *2024-02-02*

Reviewed: *2024-06-28 (undisclosed name); 2024-07-23 (undisclosed name)*

Accepted: *2024-09-10*